

Crystal orientation dependence of anelastic relaxation in 8Y-fully stabilized zirconia

Yasuhiro Okada · Masahito Matsuzawa ·
Susumu Horibe

Received: 24 January 2006 / Accepted: 2 October 2006 / Published online: 4 April 2007
© Springer Science+Business Media, LLC 2007

Abstract Mechanical loss (internal friction) in cubic zirconia was measured in the flexural mode in order to understand the local structure associated with oxygen vacancy. Polycrystal and single crystal with different orientation of longitudinal axis ($\langle 100 \rangle$, $\langle 110 \rangle$, $\langle 111 \rangle$) were adopted from 8 mol.% Y_2O_3 stabilized zirconia (8Y-FSZ), which shows that the internal friction profile depends on crystal orientation. In the present study, furthermore, anelastic strain behavior was also investigated in the single crystal specimens. Anelastic strain productivity is also strongly dependent on crystal orientation like internal friction: $\langle 100 \rangle < \langle 110 \rangle < \langle 111 \rangle$. It is considered that the crystal orientation dependence of internal friction and anelasticity is closely correlated with the behavior of cation–oxygen vacancy complexes. Finally, the mechanism of anelasticity was discussed.

Introduction

Internal friction (e.g. mechanical or dielectric loss) gives us important information on the inner structure of materials. As is well known, therefore, the measurement of internal friction is very effective for the investigation of point

defects or complexes, e.g. associated with localized elastic or electric dipole in materials [1–5]. Thermally activated reorientation of (anisotropic) dipoles in alternating stress fields (mechanical or electrical oscillations) gives rise to loss maximum. Weller [1] measured the mechanical loss in a cubic single crystal stabilized with 10 mol.% Y_2O_3 and 16 mol.% CaO, and suggested that oxygen vacancy might be positioned at one of eight nearest neighboring sites around the dopant ion with $\langle 111 \rangle$ orientation of the dipole axis in each case. Thermally activated jumps of vacancy (induced by mechanical stress) corresponding to reorientation of the $\langle 111 \rangle$ dipole axis leads to the loss maximum. Kirimoto et al. [2] examined the attenuation of longitudinal ultrasonic sound waves in the Y-FSZ single crystal doped with 9.6 mol.% Y_2O_3 . They also suggested that the effect of the longitudinal acoustic strain is to distort the environment of each oxygen site, hence modifying the effective activation energy for hopping between sites, which induces relaxation and causes attenuation of the incident wave. Although internal friction in zirconia ceramics including oxygen vacancy has been studied from the view point of material structure by many researchers [1–5], a detailed behavior of the localized structure has not yet been resolved completely.

Several years ago, our group detected a unique anelastic relaxation behavior in Y_2O_3 doped zirconia ceramics [6, 7]. When an abrupt stress is applied to the material, the strain is not induced immediately, but is formed over a period of time. Subsequently, this strain produced during loading is gradually recovered to attain the original level after unloading. This recoverable strain, that is, anelastic strain is supposed to release any stress concentration that might lead to fatal damage in the brittle material [8, 9]. Therefore, anelasticity is regarded as the most effective strengthening-toughening mechanism and an explanation of the anelastic

Y. Okada · M. Matsuzawa · S. Horibe (✉)
Department of Materials Science and Engineering, Waseda
University, 3-4-1, Ohkubo, Shinjuku-ku, Tokyo 169-8555, Japan
e-mail: horibe@waseda.jp

Present Address:
M. Matsuzawa
Material Development Section, Kyocera Corporation, 1810,
Taki-cho, Satsumasendai, Kagoshima 895-0292, Japan
e-mail: masahito.matsuzawa.cy@kyocera.jp

strain production mechanism is needed for the development of highly strengthened and toughened ceramics. In our recent work [10], we investigated anelastic behavior in some kinds of zirconia ceramics. Although the exact mechanism of anelastic strain production is still unclear, the effectiveness of anelasticity is closely correlated with oxygen vacancies included in the zirconia matrix [10]. Therefore, it is assumed that the anelastic strain productivity could be also determined by the specific behavior of the oxygen vacancy-dopant cation dipoles or complexes which bring about the internal friction.

Further study is required to grasp the details of the localized structure causing significant anelastic relaxation. In this study, we examined (i) internal friction and (ii) anelastic behavior in the Y-FSZ single crystal in order to investigate localized structure in material and to clarify the mechanism of anelasticity.

Experimental procedure

The single crystals of 8 mol.% Y_2O_3 stabilized cubic zirconia ceramics (8Y-FSZ) were supplied by Myojo Metal Co.,Ltd., Osaka, Japan. Three kinds of samples with different crystal orientation along with longitudinal axis ($\langle 100 \rangle$, $\langle 110 \rangle$, $\langle 111 \rangle$) were prepared. The two types of samples that we formed were thin-sheet and rectangular, with dimensions of $1.5 \times 10 \times 60$ mm and $3 \times 4 \times 46$ mm, respectively. As a comparison, 8Y-FSZ polycrystal sample with the same dimensions was also adopted, which was supplied by Tohoku Ceramic Co.,Ltd., Miyagi, Japan.

Internal friction

For the measurement of internal friction, the thin-sheet specimens were used. The testing machine used in this experiment was EG-HT (Nippon Techno-Plus Co.,Ltd., Osaka, Japan). One end of the samples was fixed as a node in the testing machine and the other end was clamped in special jaws attached with pendulum, which was driven by magnetic force through the solenoid coil. The flexural oscillation was forcibly excited in the specimen and the amplitude was measured using the displacement sensor. The testing was carried out in flowing Ar gas in order to avoid the influence of oxygen or hydrosphere in the air. The internal friction was evaluated by the free decay method (ASTM E756-93).

Anelasticity

For the measurement of anelastic strain behavior, the rectangular single crystal specimens were adopted. A

four-point bending test was carried out at RT, with inner and outer spans of 10 mm and 30 mm, respectively. A desired load was applied abruptly (300 MPa/s) to the specimen in order to avoid the occurrence of anelastic strain in the loading process. The applied load was maintained at the maximum stress level for a certain time, after which it was removed abruptly and the specimen was left until the strain showed no further change. The strain was measured by a strain gauge attached to the tensile surface of the specimens as the time elapsed. The measured strain fluctuates when ambient temperature slightly changes. In order to avoid this experimental error, a dummy gauge was attached to another specimen that was not loaded. The values of the load and the strain were recorded as a voltage signal using an oscillographic recorder, and an analysis of the non-elastic strain behavior was conducted on a personal computer. The non-elastic strain, $\varepsilon_{\text{non-elastic}}$, was calculated from the following equation:

$$\varepsilon_{\text{non-elastic}} = \varepsilon_{\text{total}} - \sigma/E, \quad (1)$$

where $\varepsilon_{\text{total}}$ is the total strain and σ is the stress. E is Young's modulus, which was calculated from the slope of the stress-strain unloading curve at the lower stress level. The recoverable strain after unloading was defined as the anelastic strain.

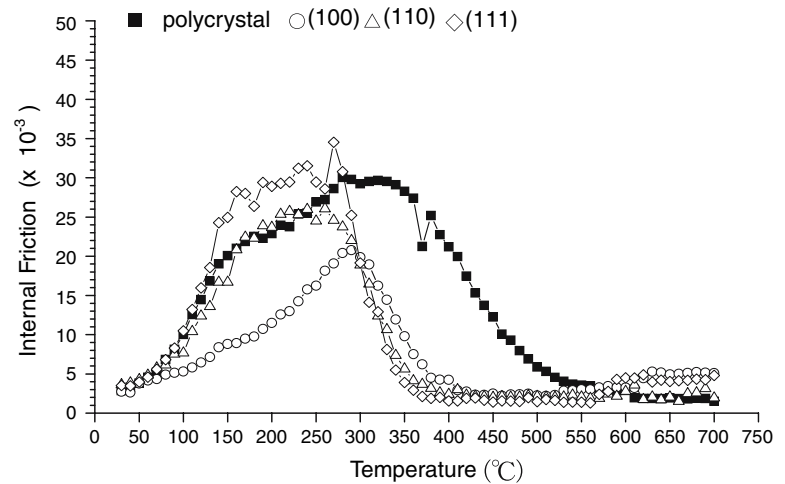
Results and discussion

Crystal orientation dependence of internal friction spectra

Figure 1 shows the relationship between internal friction and temperature for 8Y-FSZ poly- and single crystal specimens with $\langle 100 \rangle$, $\langle 110 \rangle$ and $\langle 111 \rangle$ orientation of the longitudinal axis. This figure indicates the result under the condition of flexural oscillation. The order of internal friction for each crystal orientation at 100–300 °C is; $\langle 100 \rangle < \langle 110 \rangle < \langle 111 \rangle$ under the flexural oscillation mode. As shown in Fig. 1, the internal friction spectra is composed of two peaks; one peak around 170 °C and another peak at the region of 280–310 °C. According to the dipole model [1, 3, 11], this result indicates the existence of one or more kinds of anisotropic dipoles (low defect symmetry), though the first peak (around 170 °C) is hardly observed in $\langle 100 \rangle$ orientation.

It is considered the anelastic relaxation to produce the peak of the internal friction is due to the common cause in ZrO_2 with an oxygen defect [12]. Dopant cation (Y^{3+}) is surrounded by the sites of oxygen ions corresponding to 8-fold coordination because of a fluorite structure [1, 3, 11]. The oxygen vacancy may be positioned at one of eight

Fig. 1 Temperature dependence of the internal friction in 8Y-FSZ polycrystal and single crystals for flexural oscillation. ■, ○, △, ◇ shows polycrystal and $\langle 100 \rangle$, $\langle 110 \rangle$, $\langle 111 \rangle$, respectively



nearest neighboring sites around the dopant ion with $\langle 111 \rangle$ orientation of the dipole axis (trigonal defect symmetry). Thermally activated jumps of the vacancy corresponding to reorientation of the $\langle 111 \rangle$ dipole axis leads to the internal friction peak. As for the local structure, Y–V dipole, Ohta et al. [13, 14] advocated an alternative model: Y–V–Y asymmetry local structure. They reported that in the Y–V–Y block, an oxygen vacancy is bound on either of two equivalent sites which are separated by the potential barrier between two Zr-ions in $\langle 100 \rangle$ directions by layers of Y-ions, and is stable because of charge neutrality (Refer to Fig. 5(b) in paper [13]). For 8 mol.% Y_2O_3 doped FSZ, the oxygen vacancies seem to be preferentially bound within the Y–V–Y blocks. It is considered that such a local structure could produce the first peak around 170 °C.

An oxygen vacancy hops to a nearest neighboring oxygen site by external oscillation, where the translation symmetry of the lattice is broken by the presence of the Y-ion and the potential energies due to the surrounding cations become non-equivalent due to strain. Ohta et al. [13] reported that it remains equivalent under $\langle 100 \rangle$ strain, but it becomes non-equivalent under $\langle 110 \rangle$ strain for longitudinal sound wave corresponding to our flexural oscillation. The first peak was not detected in $\langle 100 \rangle$ orientation for flexural oscillation, which means that the distortion of oxygen sites remain equivalent under this condition. In $\langle 110 \rangle$ and $\langle 111 \rangle$ orientations, on the other hand, the equivalent state is broken and further hopping of oxygen vacancies is required. It may be that such a further hopping of oxygen vacancies results in the first peak. Ozawa et al. [12] also found that the internal friction peak in 2Y-TZP is not described by a single Debye peak and suggested the appearance of complex relaxation processes which produce a broad peak. Various clusters (Y–V, Zr–V, Y–V–Y etc.) with lower defect symmetry may become more complicated and the vacancies will have unknown possibilities for a final hopping site.

The increase of internal friction around over 580 °C is detected only in single crystal specimens, though indefinite in $\langle 110 \rangle$ direction. Microcracking is suspected to be one of the reasons for this phenomenon. Weller et al. [3] also detected the rapid increase of internal friction around over 1127 °C in the 8Y-FSZ polycrystal and the less increase in the single crystals of 10Y-FSZ. They explained these phenomena in terms of the typical one in the phase transition. Therefore, there is a possibility that the phase transition might occur even in the present 8Y-FSZ single crystal. Ruhle and Evans [15] confirmed that microcracks occur within regions of local residual tension, caused by thermal expansion mismatch and/or by transformation. Once a microcrack is nucleated, it is unlikely that the microcracks will disappear during the imposed thermal cycles. The damping effects of cracks in a single crystal sample will therefore develop and increase with the number of thermal cycles [4]. When this test reaches the high-temperature range, many of our 8Y-FSZ single crystal samples progressively degrade under the repeated impulse excitation. In this study, therefore, it seems that the microcracking might occur by the phase transition at the high temperature. Conversely, the rise of the internal friction in the polycrystal is not observed in the temperature region measured. At a further high temperature, viscoelastic damping could arise from the glide/climb motion of intragranular dislocations or from grain boundary sliding [16]. Therefore, the internal friction could rise at a further high temperature. Some rapid rises of a viscoelastic internal friction are actually reported at temperatures over 900 °C [3, 16].

The relationship between anelasticity and localized structure

Figure 2 shows the non-elastic behavior in three kinds of samples with different crystal orientation at 100 MPa and a

load-holding time of 1 h. Non-elastic strain produced in each sample is all composed of anelastic strain because most non-elastic strain is recovered after unloading. Clearly, it is found that non-elastic behavior, i.e. anelastic property, is different and strongly depends on the crystal orientation, as well as the internal friction. Anelastic strain is produced most effectively at $\langle 111 \rangle$ orientation. Yet at $\langle 100 \rangle$ orientation, it seems hard to produce anelastic strain. Although saturation is still not attained only after 1 h holding, the order of anelastic productivity is regarded as follows; $\langle 100 \rangle < \langle 110 \rangle < \langle 111 \rangle$. (Time holding longer than 1 h for the accurate measurement of micro-strain could not be conducted because of various types of electrical noise.) From Fig. 2, as the major points, the mean values of anelastic strain produced after 5 min, 30 min and 1 h are about 14, 22 and 25 $\mu\epsilon$, respectively. These values exactly correspond with the data of 8Y-FSZ polycrystalline samples in our previous paper [10], suggesting that anelasticity in polycrystals must be composed of a simple addition of anelastic strain produced in each grain. Young's modulus is sharply different in each orientation (See Table 1). Therefore, "true" anelastic strain productivity must be evaluated as a ratio of anelastic strain to elastic strain ($\epsilon_{an}/\epsilon_{elastic}$). These values after time-elapses of 5 min, 30 min and 1 h are summarized in Table 2(a)–(c), respectively. (Young's modulus adopted here was directly calculated from the slope of the stress-strain curve.) The same ten-

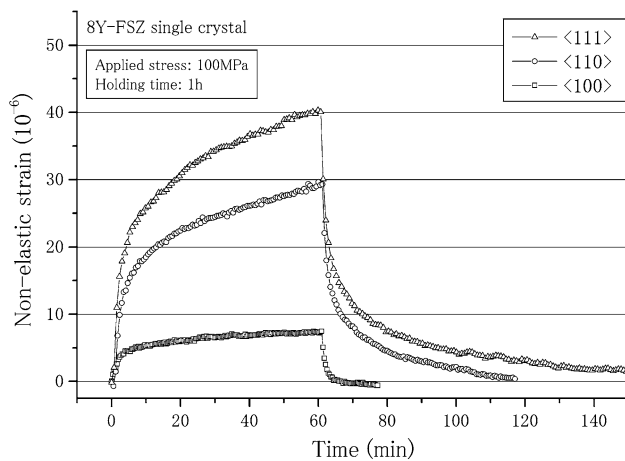


Fig. 2 Non-elastic strain behavior for 8Y-FSZ single crystal with different orientation at 100 MPa and a load-holding time of 1 h

Table 1 Young's modulus for each crystal orientation at RT

Orientation	Young's modulus (GPa)
poly	215
$\langle 111 \rangle$	149
$\langle 110 \rangle$	172
$\langle 100 \rangle$	319

dency of anelastic productivity; $\langle 100 \rangle < \langle 110 \rangle < \langle 111 \rangle$; is also confirmed by this ideal evaluation.

In our previous study [10], we concluded that the anelastic property is closely correlated with the existence of oxygen vacancies included in the zirconia matrix. Actually, it has been confirmed that the anelastic property of Ce-TZP was extremely enhanced by the increase of oxygen vacancies. However, we concluded that the extent of anelasticity cannot be determined only by the number of oxygen vacancies. Therefore, it is assumed that the incidence of anelasticity may be related to the ionic radius, ionic valence, configuration of oxygen vacancies and so on. If there is not any interaction at all between oxygen vacancy and other structural ions in the matrix, anelastic productivity should not depend on crystal orientation unlike Fig. 2. Weller and Schubert [17] have examined internal friction and dielectric loss in 3Y-TZP and asserted that Y ion–oxygen vacancy dipoles exist which possess trigonal symmetry (i.e. are oriented parallel to $\langle 111 \rangle$ direction), causing anelastic relaxation (internal friction). It should be noted, in the present study, that the crystal orientation dependence of anelastic productivity corresponds to that of internal friction. This result suggests a possible link between anelastic behavior and cation–oxygen vacancy dipoles (Y–V dipoles).

The ratio of anelastic strain productivity of $\langle 100 \rangle$ and $\langle 110 \rangle$ to that of $\langle 111 \rangle$ is calculated in the end column on Table 2(a)–(c). Note that these ratios do not depend on the time-elapse of load holding. It is unlikely that a certain direction can produce anelastic strain more effectively than the other two directions. The order of the producing speed would not change even after long time elapse, which suggests that there is a significant link between the crystal orientation and the anelastic strain producing speed. In other words, this interesting tendency suggests that anelastic strain might be produced by a sole factor

Table 2 The data of anelastic strain behavior from Fig. 2

Orientation	$\epsilon_{an}(\mu\epsilon)$	$\epsilon_{elastic}(\mu\epsilon)$	$\epsilon_{an}/\epsilon_{elastic}(\%)$	The ratio of anelastic strain productivity
(a) 100 MPa—after 5 min				
$\langle 111 \rangle$	22	654	3.4	1.00
$\langle 110 \rangle$	16	565	2.8	0.84
$\langle 100 \rangle$	4.5	292	1.5	0.46
(b) 100 MPa—after 30 min				
$\langle 111 \rangle$	34	654	5.2	1.00
$\langle 110 \rangle$	24	565	4.3	0.82
$\langle 100 \rangle$	7	292	2.4	0.46
(c) 100 MPa—after 1 h				
$\langle 111 \rangle$	40	654	6.1	1.00
$\langle 110 \rangle$	30	565	5.3	0.87
$\langle 100 \rangle$	8	292	2.7	0.44

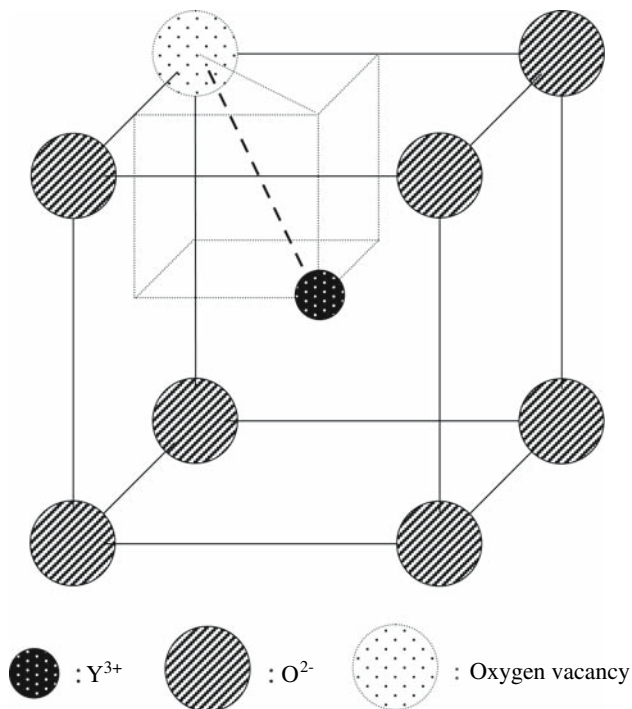


Fig. 3 Atomic model for defect (Yttrium–Oxygen vacancy dipole)

(mechanism), not by some complicated local structures. As mentioned before, the behavior of the Y–V dipole along with $\langle 111 \rangle$ orientation is the most possible mechanism of anelasticity. Provided the Y–V dipole is distorted by certain amount of distance, the proportion of distortion for each orientation $\langle 111 \rangle$, $\langle 110 \rangle$ and $\langle 100 \rangle$ is $\sqrt{3} : \sqrt{2} : 1$ (i.e. 1:0.82:0.58), as shown in Fig. 3. This proportion nearly corresponds to that of the ratio of anelastic strain productivity in Table 2, which suggests that anelastic strain behavior is closely linked with Y–V dipoles. From the present study, we can insist that anelastic strain should be mainly produced by a slight shift of ions along with $\langle 111 \rangle$ cation–oxygen vacancy dipole.

Conclusion

Based on the research of internal friction and anelasticity in 8Y-FSZ poly- and single-crystals, the following conclusions are obtained;

1. The order of internal friction for each crystal orientation at RT is; $\langle 100 \rangle < \langle 110 \rangle < \langle 111 \rangle$ under the flexural oscillation mode.
2. The non-elastic behavior, i.e. anelastic property, strongly depends on crystal orientation, as well as the internal friction. The order of anelastic productivity is regarded as follows; $\langle 100 \rangle < \langle 110 \rangle < \langle 111 \rangle$.

The crystal orientation dependence of internal friction and anelasticity is closely correlated with the behavior of cation–oxygen vacancy complexes. It is assumed that anelastic strain should be mainly produced by a slight shift of ions along with $\langle 111 \rangle$ cation–oxygen vacancy dipole.

Acknowledgements This research was supported by: (1) Grant-in-Aid for Open Research Center Project by the Ministry of Education, Culture, Sports, Science and Technology (MEXT) of the Japanese Government and (2) Waseda University Grant for Special Research Projects (2005B-192). The authors wish to acknowledge these supports.

References

1. Weller M (1993) *Z Metallkd.* 84:381
2. Kirimoto K, Nobugai K, Miyasato T (1999) *J Jpn Appl Phys* 38:6526
3. Weller M, Damson B, Lakki A (2000) *J Alloy Compound* 310:47
4. Roebben G, Basu B, Vleugels J, Van der Biest O (2003) *J Europ Ceram* 23:481
5. Matsusita K, Okamoto T, Shimada M (1985) *J de Physique Colloque, Supplement* 46:C10-549
6. Pan LS, Horibe S (1996) *J Mater Sci* 31:6527
7. Pan LS, Horibe S (1997) *Acta Mater* 45:463
8. Matsuzawa M, Sato F, Horibe S (2001) *J Mater Sci* 36:2491
9. Matsuzawa M, Horibe S (2002) *Mater Sci Eng A* 333:199
10. Matsuzawa M, Horibe S (2003) *Mater Sci Eng A* 346:75
11. Weller M (1996) *J de Physique IV* 6:C8
12. Ozawa M, Hatanaka T, Hasegawa H (1991) *J Jpn Ceram Soc* 99:643
13. Ohta M, Kirimoto K, Nobugai K (2001) *Jpn J Appl Phys* 40:5377
14. Ohta M, Kirimoto K, Nobugai K, Wigmore JK, Miyasato T (1989) *Physica B* 316–317:5
15. Ruhle M, Evans AG (1989) *Prog Mater Sci* 33:85
16. Lakki A, Herzog R, Weller M, Schubert H, Reetz C, Görke O, Kilo M, Borchardt G (2000) *J Europ Ceram* 20:285
17. Weller M, Shubert H (1986) *J Am Ceram Soc* 69:573